ACADEMIC PRESS

Available online at www.sciencedirect.com

SCIENCE DIRECT®

Journal of Sound and Vibration 264 (2003) 835–850

JOURNAL OF SOUND AND VIBRATION

www.elsevier.com/locate/jsvi

Adaptive non-linear control of a clamped rectangular plate with PZT patches

Kougen Ma*

German Aerospace Center (DLR), Institute of Structural Mechanics, Lilienthalplatz 7, 38108, Braunschweig, Germany

Received 24 August 2001; accepted 22 July 2002

Abstract

The dynamic behavior and control of a clamped rectangular plate with bonded piezoelectric ceramic patches are investigated in this paper. The dynamic behavior is studied experimentally, showing that the plate exhibits dense modes, varying residual stress and non-linearity. An adaptive non-linear control scheme is then presented, which introduces a non-linear function into the normal adaptive feedforward control to non-linearize a reference signal. Vibration reductions using both the normal adaptive feedforward control and the adaptive non-linear control are compared in the cases of sinusoidal excitations at the first nine modal frequencies of the plate and a swept-frequency harmonic excitation below 100 Hz, indicating that the adaptive non-linear control can suppress not only the fundamental frequency vibration that the normal adaptive feedforward control can only attenuate, but also its higher harmonic components. Significant vibration reduction achieved by the adaptive non-linear control demonstrates its validity and reliability.

1. Introduction

Smart structure technologies deal with sophisticated aspects of sensors, actuators, control and signal processing. It involves multi-discipline knowledge, such as mechanics, physics, mechanical engineering, control, and computers. Because of its large potential applications in the fields of aerospace, civil engineering, shipbuilding, automobile, precision instruments, and machines, it has been developed rapidly. For example, smart wings can provide more lift and/or better aero-elastic dynamic performance by driving integrated actuators to change the curvature of a profile or the

*Corresponding author. Present address: Intelligent and Composite Materials Laboratory, Department of Mechanical Engineering, University of Hawaii at Manoa, 2540 Dole Street, Holmes 302, Honolulu, HI 96822, USA. Tel.: +1-808-956-7946.

E-mail address: kougen@wiliki.eng.hawaii.edu (K. Ma).

0022-460X/03/$ - see front matter
doi:10.1016/S0022-460X(02)01220-8

leading- and trailing-edge angles of an airfoil. Smart rotors can have less vibration load and longer fatigue-life. Among various smart structures, smart structures with piezoelectric ceramic patches have received much attention in recent years, due to the fact that piezoelectric ceramic materials have mechanical simplicity, small volume, light weight, large bandwidth, efficient conversion between electrical and mechanical energy, and abilities of performing shape and vibration control and being easily integrated into structures.

Smart structures may be time-variant and non-linear. It is a challenge to control such structures. Conventional active controller design methods, e.g., eigenstructure assignment and optimal control, require accurate mathematical models. But accurate models are almost impossible for smart structures, because of non-ideal behavior, simplifications in modelling, manufacture error, parts wear, and environment change. In this case, adaptive control may be an attractive alternative.

There are two radically different adaptive control approaches: adaptive feedback control [1] and adaptive feedforward control. Adaptive feedforward control was originally used for noise control [2–4] and then extended to vibration control. Up to now, it has been studied in large space structure control [5], civil structure vibration under seismic [6] or wind excitation [7], helicopter vibration control [8], wing flutter suppression [9], and vibration reduction for automobiles [10]. Its recursive capability makes it very suitable for digital signal processors (DSP). In the meantime, the rapid development of digital signal processors also expedites the application of this technology.

In terms of analysis and control of plates with piezoelectric ceramic materials, much work have been done dealing with various geometric sizes, boundary conditions, PZT materials, control methods, though most of them just considered linear and time-invariant plates. Lammering et al. [11] investigated a rectangular steel plate ($600 \times 500 \times 2\,\mathrm{mm}^3$) supported by four screw joints. Two small piezoelectric patches were bonded to the center of the lower and upper surfaces. A method was presented that did not require special finite elements for the analysis of structures with piezoelectric devices, but which used conventional finite elements. A qualitative good agreement of the frequency response function was obtained between the experimental and the numerical results. There were three modes below 100 Hz. Lim et al. [12] developed a procedure to design an optimal output feedback controller. In the procedure, a common finite element formulation for the dynamic response of a piezoelectric material was employed. A modal analysis was then conducted, and some of modal co-ordinates were selected to form a modal state space model. Based on this modal state space model, an optimal output feedback controller was designed. The procedure was applied to a clamped square aluminum plate ($305 \times 305 \times 0.8\,\mathrm{mm}^3$) with five pair collocated piezoelectric ceramic sensors and actuators. Dynamic analysis and control system simulations were performed. Suk-Yoon Hong et al. [13] investigated coupled mode optimal control of the same plate as in Ref. [12] using approximately normalized eigenfunctions. The first six modal responses were simulated. Instead of the optimal output feedback control in Ref. [12], Chen et al. [14] utilized the independent modal space control (IMSC) method. Modal sensors and actuators were proposed. A cantilevered aluminum plate ($350 \times 50 \times 1.59\,\mathrm{mm}^3$) with eight piezoelectric ceramic patches for modal sensors and three piezoelectric ceramic patches for modal actuators was chosen as a numerical example. The number of modes below 100 Hz was two. In Ref. [15], a 2-degree-of-freedom model was constructed for a structural dynamic system consisting of a linear elastic plate with bonded piezoelectric ceramic sensors/actuators. Rate-feedback

control, hybrid fuzzy-PID control, genetic algorithm-designed PID control and linear quadratic Gaussian/loop transfer recovery (LQR/LTR) control were studied on a clamped rectangular aluminum plate ($711 \times 533 \times 1.27\,mm^3$) with five pair of collocated piezoelectric ceramic patches. It provided an appropriate framework for optimization and robustness studies of vibration control of flexible structures. The number of modes below 100 Hz is four. Chantalakhana and Stanway [16] studied a clamped–clamped aluminum plate with one or two piezoelectric ceramic patches as actuators to realize active constrained layer damping. Modal control was employed. The number of modes below 100 Hz is two. Piezoelectric stack actuators were also used in Refs. [17,18] to control the vibration of plates. A Kalman-estimator-based feedforward controller and two support configurations were studied in Ref. [17]. In Ref. [18], four piezoelectric stack actuators were located at each corner of the plate and optimal control was employed. The number of modes below 100 Hz was seven.

This investigation will focus on the adaptive non-linear control of plate structures using piezoelectric ceramic sensors and actuators. A typical structure is considered here which consists of a series of thin panels that are clamped around their individual boundaries by a continuous metal frame. This typical structure can often be found in spacecrafts, launch vehicles, and automobiles. It may exhibit dense modes, time-variant characteristics and non-linearity because of its large size and small thickness. The paper includes five sections. First, the dynamics of the plate is studied experimentally. An adaptive non-linear control scheme is then presented in Section 2. In Section 3, the validity and reliability of the proposed scheme are investigated, and comparison is made between the normal adaptive feedforward controller and the adaptive non-linear controller.

2. The dynamics of the experimental plate

Fig. 1 shows a rectangular steel plate with eight bonded piezoelectric ceramic patches. Its dimension is $900 \times 600 \times 0.9\,mm^3$. The used piezoelectric ceramic patch is Sonox P53 with NiPt electrodes, 0.2 mm in thickness, 25 mm in width, 50 mm in length and 2.7 g in weight. Four of them, denoted as S1–S4, are bonded on the upper surface as sensors, and the rest, named A1–A4, collocated on the lower surface as actuators. The plate is clamped fully on its four edges by a strong steel frame, as shown in Fig. 2.

First, the dynamic responses induced by an external disturbance (i.e., the dynamic responses of the primary paths) are investigated. A shaker at point P1 of Fig. 1 is used to excite the plate. The spectra of the sensors S3 and S4, as shown in Fig. 3, illustrate that there are 10 modes below 100 Hz, indicating dense modes of the plate. During measurement, it was also observed that the resonant frequencies vary from time to time. Fig. 4 shows the frequency response function between the sensor S1 and the shaker at different measuring times, demonstrating the large variation of the first resonant frequency. Curve 1 in Fig. 4 was measured at 12:45 am. Keeping on vibrating the plate, curves 2–8 were measured at 1:15, 1:45, 2:15, 2:25, 2:40, 2:50, and 3:10 pm, respectively. The first resonant frequency of the plate gradually decreases from 29.25 to 25.4 Hz (curves 1–6) with the excitation duration and tends to be steady after long-time vibration (curves 6–8). It has been learned that the cause of the variation of the natural frequencies is the pre-stress distribution of the plate. Because the plate is so large and thin, with clamped boundary condition, pre-stress is inevitable. The vibration changes the distribution of the pre-stress, and results in the

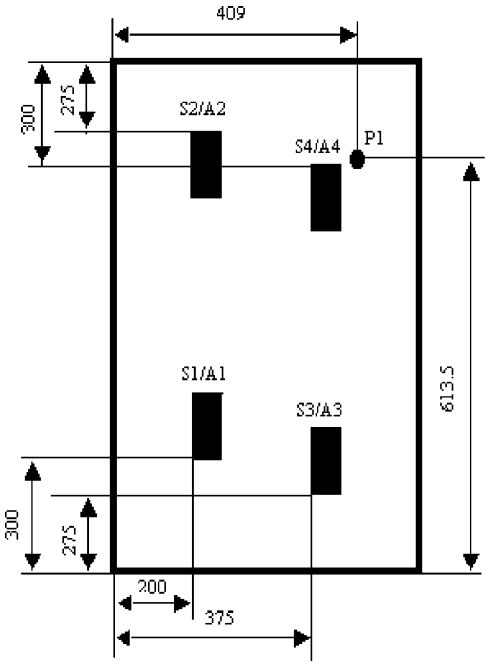

Fig. 1. The plate.

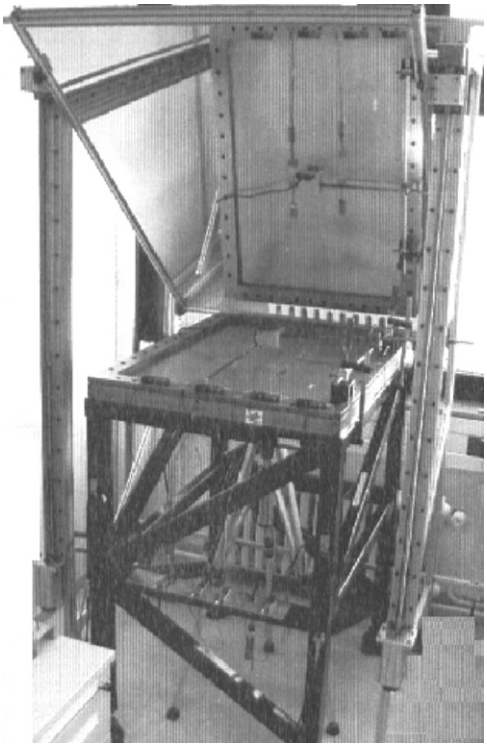

Fig. 2. The experimental plate.

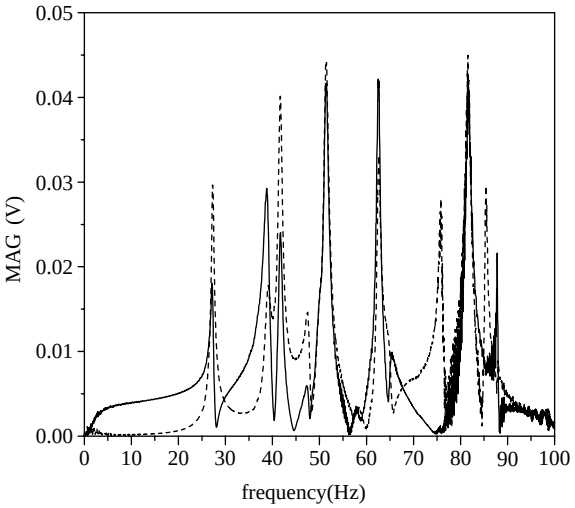

Fig. 3. The spectra of the sensors S3 and S4:----, sensor S3; ——, sensor S4.

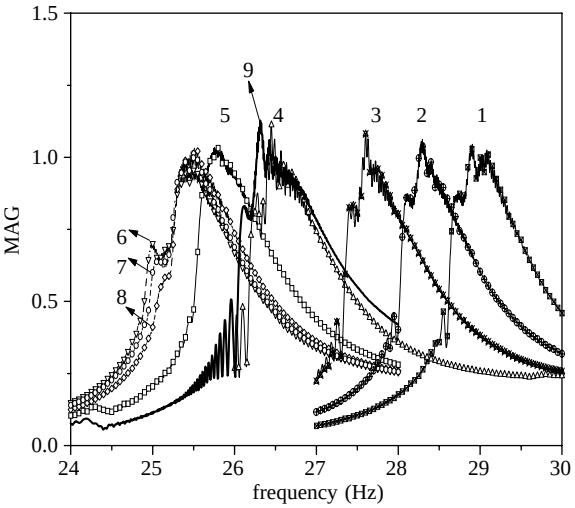

Fig. 4. The variation of the first modal frequency: -·-, 12:45; -·-, 13:15; -·-, 13:45; —△—, 14:15; —□—, 14:25; --▽--, 14:40; ---○---, 14:50; ---○---, 14:10; ——, 15:55:

variation of the natural frequencies. The natural frequencies tend to be steady, while the pre-stress is well distributed. In addition, it is also found that the resonant frequencies of the plate vary immediately, if the well-distributed stress is disrupted. Curve 9 in Fig. 4 shows this immediate change of the first resonant frequency after the plate was hit by a hammer at 3:55 pm, resulting in the change of the first resonant frequency from 25.4 to 26.3 Hz. The effect of the pre-stress on resonant frequencies has also been verified by finite element analysis considering the pre-stress in Ref. [19].

Next, the frequency response functions of the secondary paths are measured and shown in Fig. 5. In this figure, $S_{ij}(i,j=1,2,3,4)$ denotes the frequency response functions between the jth

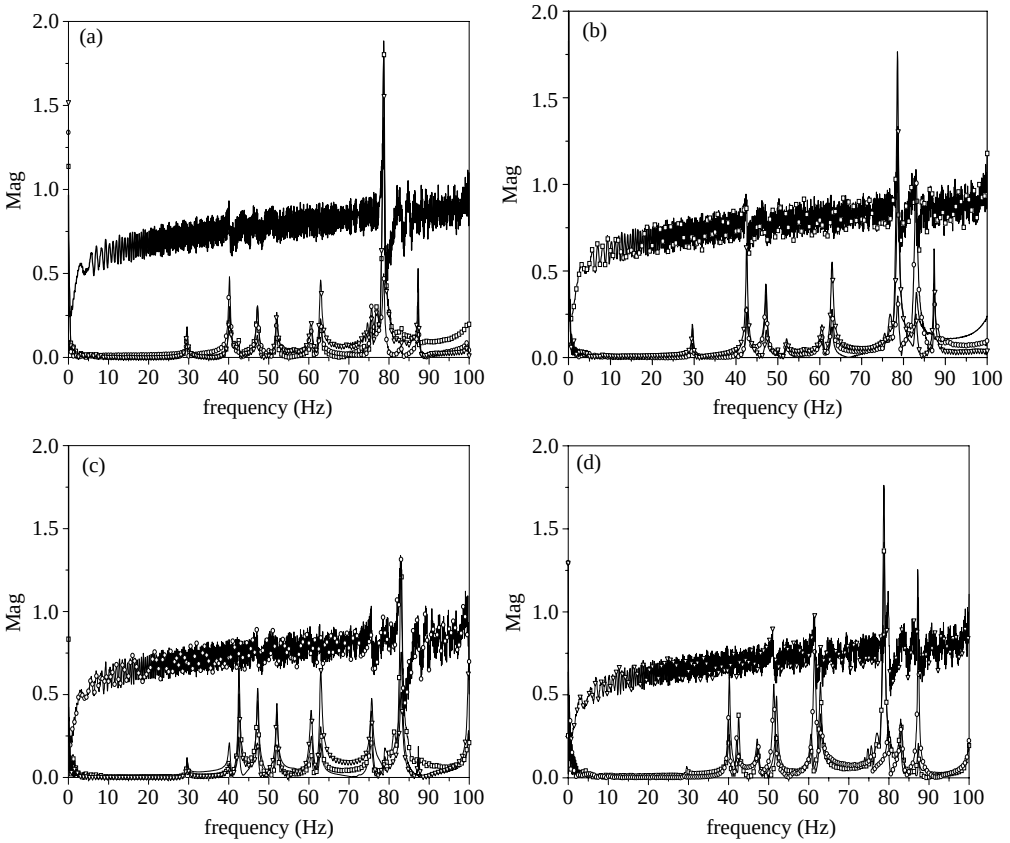

Fig. 5. Frequency response functions between different actuators and sensors. (a) Actuator A1: ——, S_{11}; —□—, S_{21}; —○—, S_{31}; —▽—, S_{41}. (b) Actuator A2: ——, S_{12}; —□—, S_{22}; —○—, S_{32}; —▽—, S_{42}. (c) Actuator A3: ——, S_{13}; —□—, S_{23}; —○—, S_{33}; —▽—, S_{43}. (d) Actuator A4: ——, S_{14}; —□—, S_{24}; —○—, S_{34}; —▽—, S_{44}.

actuator (A_j) and the ith sensor (S_i). It is demonstrated that the piezoelectric ceramic actuators affect the response of the collocated piezoelectric ceramic sensors greatly, but weakly for the non-collocated piezoelectric ceramic sensors, especially in the low frequency range. This means that the effectiveness of actuators may be localized.

Non-linearity is inherent, because the plate is large and thin. Figs. 6 and 7 present the existence of non-linearity. Fig. 6 shows the power spectra of the sensors S2 and S3 under a sinusoidal excitation at the frequency of 30.2 Hz through the actuator A1. Higher harmonic components clearly appear and some are even larger than the fundamental component at some positions, e.g., at the position of the sensor S3. Fig. 7 gives the frequency response functions between the piezoelectric ceramic sensor S1 and the actuator A1 for different actuator amplitudes. It shows that the collocated sensor amplitude decreases while the collocated actuator amplitude rises. It could be that the large actuator amplitude generates a large deformation in the neighborhood of the actuator, resulting in a strong non-linearity and a small fundamental component.

Summarizing the above results, the plate has dense modes, is time-variant and non-linear.

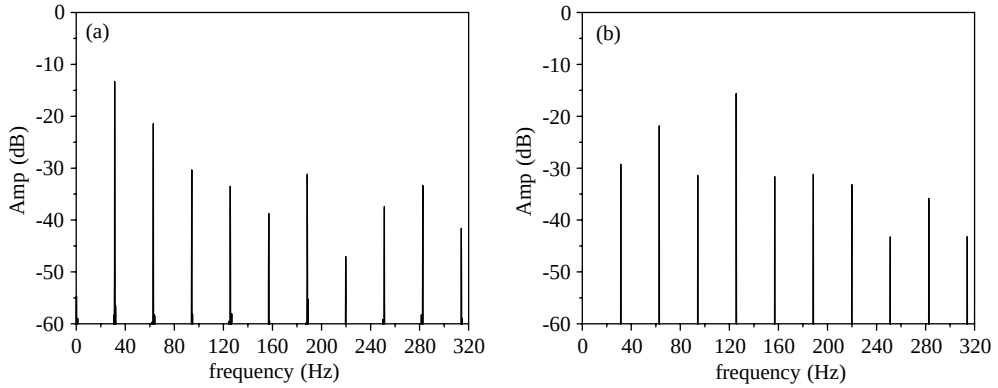

Fig. 6. The power spectra of the sensors S2 and S3 under a sinusoidal excitation at the frequency of 30.2 Hz: (a) sensor S2, (b) sensor S3.

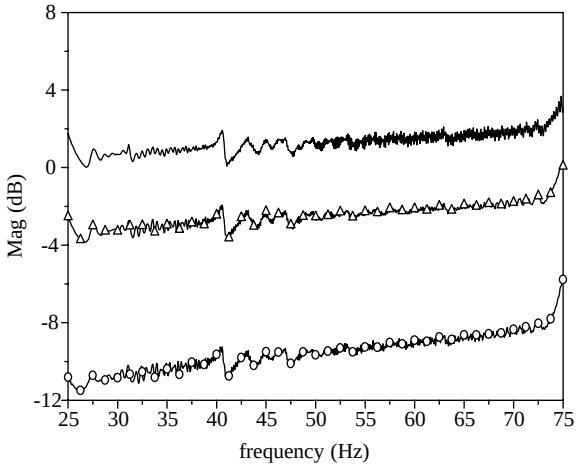

Fig. 7. The frequency response function between the sensor S1 and the actuator A1: ——, 0.5 V; —△—, 1 V; —○—, 2 V.

3. Adaptive non-linear control

The responses of the sensors S1–S4 in frequency domain can be written as

$$\begin{Bmatrix} E_1(s) \\ E_2(s) \\ E_3(s) \\ E_4(s) \end{Bmatrix} = \begin{bmatrix} S_{11} & S_{12} & S_{13} & S_{14} \\ S_{21} & S_{22} & S_{23} & S_{24} \\ S_{31} & S_{32} & S_{33} & S_{34} \\ S_{41} & S_{42} & S_{43} & S_{44} \end{bmatrix} \begin{Bmatrix} U_1(s) \\ U_2(s) \\ U_3(s) \\ U_4(s) \end{Bmatrix} + \begin{Bmatrix} P_1 \\ P_2 \\ P_3 \\ P_4 \end{Bmatrix} D(s), \tag{1}$$

i.e.,

$$\mathbf{E}(s) = \mathbf{S}\mathbf{U}(s) + \mathbf{P}D(\mathrm{s}), \tag{2}$$

where $E_i(s)$ $(i = 1, 2, 3, 4)$, $U_j(s)$ $(j = 1, 2, 3, 4)$ and $D(s)$ are the Laplace transforms of the responses of the sensors S1–S4 $e_i(t)$, the control signals of the actuator A1–A4 $u_j(t)$ and the external disturbance $d(t)$, respectively. S_{ij} $(i,j = 1, 2, 3, 4)$ and P_i $(i = 1, 2, 3, 4)$ are transfer functions of the secondary paths and the primary paths of the plate.

Eq. (1) can also be written in the time domain

$$e_i(k) = \sum_{j=1}^{4} \sum_{n=1}^{N} s_{ij}(n) u_j(k - n + 1) + \sum_{m=1}^{M} p_i(m) d(k - m + 1), \tag{3}$$

in which s_{ij}, p_i are the impulse responses of the transfer functions S_{ij} and P_i in lengths of N and M, respectively.

3.1. Adaptive feedforward control

The principle of adaptive feedforward control is drawn in Fig. 8. Its evident feature is the introduction of a so-called reference signal **X**, which is an external signal correlated with the external disturbance **D**. The objective of adaptive feedforward control is to tune the controller **W** adaptively to drive the error **E** to minimum (ideally zero).

Control signal u_j is usually written as the convolution of the controller weight w_j and the reference signal, i.e.,

$$u_j(k) = \sum_{l=1}^{L} w_{jl} x(k - l + 1), \tag{4}$$

where L is the length of the impulse response of the controller, and x is the reference signal. Substituting Eq. (4) into Eq. (3), yielding

$$\begin{aligned} e_i(k) &= \sum_{m=1}^{M} p_i(m) d(k - m + 1) + \sum_{j=1}^{4} \sum_{n=1}^{N} s_{ij}(n) \sum_{l=1}^{L} w_{jl} x(k - n - l + 2) \\ &= \sum_{m=1}^{M} p_i(m) d(k - m + 1) + \sum_{j=1}^{4} \sum_{l=1}^{L} w_{jl} r_{ij}(k - l + 1), \end{aligned} \tag{5}$$

where

$$r_{ij}(k) = \sum_{n=1}^{N} s_{ij}(n) x(k - n + 1) \tag{6}$$

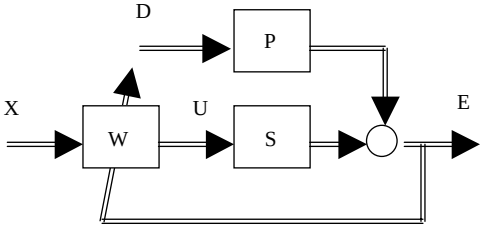

Fig. 8. Adaptive feedforward control.

is called the filtered-x signal. In practice, for calculating $r_{ij}(k)$, $s_{ij}(n)$ has to be estimated on-line or off-line [20], i.e., $s_{ij}(n)$ in Eq. (6) must therefore be replaced by $\hat{s}_{ij}(n)$.

How to adjust the controller is very important in this control method. It depends on controlled structures, disturbance, complexity of algorithms, and the hardware of computer control systems. There are many adaptive filtering algorithms, e.g., the least mean square (LMS) algorithm, the recursive least square (RLS) algorithm, the fast transversal filtering algorithm (FTF) and the gradient-based least square (GLS) algorithm. The LMS algorithm requires little calculation, but the normal LMS algorithm converges slowly. The RLS algorithm requires a little more calculation than for the LMS algorithm for a low order filter, but it can produce a faster convergence. The GLS algorithm takes advantages of both the LMS and the RLS algorithms, and can provide small computational complexity and quick convergence rate [20].

The LMS algorithm is widely used because of its low computation cost. Its cost function is

$$J(k) = \sum_{i=1}^{4} e_i^2(k). \tag{7}$$

The controller weight can be recursive by

$$w_{jl}(k+1) = w_{jl}(k) + \mu \frac{\partial J(k)}{\partial w_{jl}}, \tag{8}$$

$$\frac{\partial J(k)}{\partial w_{jl}} = 2 \sum_{i=1}^{4} e_i(k) r_{ij}(k-l+1), \tag{9}$$

where μ is the convergence factor.

For the plate, the lengths of the impulse responses of the transfer functions S_{ij} and the controller are set as 400 and 300, respectively, and the sampling frequency is set as 1000 Hz. As mentioned above, there are four sensors and four actuators in the plate. Adaptive feedforward control was supposed to be realized in the dSPACE real-time control system, unfortunately, it could not bear so much computation. A simplification of the controller configuration is needed to make real-time computation possible.

Here, advantage is taken of the fact that the piezoelectric ceramic actuators have very weak effects on the responses of the non-collocated piezoelectric ceramic sensors. This fact means that the diagonal elements in the **S** matrix of Eq. (1) are larger than the off-diagonal elements, and the off-diagonal elements may be neglected. Using this feature results in the following two benefits. First, this neglect decreases the computational complexity greatly. The computation of the filtered-x signals is reduced to 25% of its previous amount, because only r_{ii} $(i = 1, 2, 3, 4)$ are computed in Eq. (6); moreover, much computation is saved in the adaptation of Eqs. (8) and (9). Second, this neglect results in a decentralized adaptive feedforward control strategy, and each decentralized adaptive control subsystem consists of one pair of collocated piezoelectric ceramic sensor and actuator. It is well known that collocated sensors and actuators are advantageous from the viewpoint of stability [12].

Fig. 9 depicts the configuration of the control system, which consists of the plate, SVR150-3 (3 channels) and LE150/025 (1 channel) amplifiers for the piezoelectric ceramic actuators with 50 V DC offset, four Kemo analog low-pass filters with cut-off frequency 200 Hz, a shaker and its amplifier, ONO SOKKI FFT analyzer and the dSPACE real-time control system. The plate is

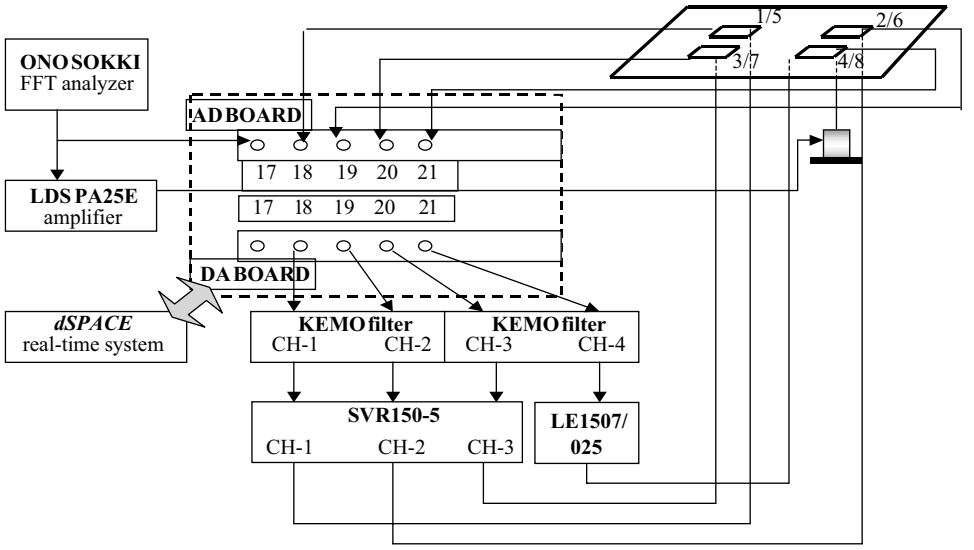

Fig. 9. The configuration of the control system.

excited by the shaker using a sinusoidal signal generated by the ONO SOKKI FFT analyzer at the frequencies of the different modal frequencies of the plate. This sinusoidal signal is also taken as the reference signal.

Fig. 10 shows the responses of the sensor S1 under sinusoidal excitations at the first four modal frequencies, respectively. Because of the non-linearity, each response contains higher harmonic components. From this figure, it is concluded that the control results are not satisfactory. Table 1 lists the amplitudes of the power spectra. It can be seen that the fundamental component is almost suppressed by the adaptive feedforward controller (AFC) for each modal frequency excitation, but the higher harmonic components remain, even are slightly enhanced. It indicates that the adaptive feedforward controller is not capable of reducing the higher harmonic components.

3.2. *Adaptive non-linear control*

Adaptive feedforward control is not available to control the higher harmonic components in responses. This is just because the reference signal does not correlate with the higher harmonic components in these responses. In order to solve this problem, one idea proposed here is to introduce a non-linear functional block into the adaptive feedforward control strategy. This non-linear functional block must have the following capability: it receives an input reference signal that only contains the fundamental component and its output contains both the fundamental and higher harmonic components, i.e., it can non-linearize the reference signal. The schematic diagram of this control scheme is drawn in Fig. 11. The non-linear functional block may be a polynomial or other ordinary non-linear functions, e.g., saturation. Here a polynomial is used, that is

$$f(x; a_i, k) = \sum_{i=1}^{NN} a_i x^i(k), \tag{10}$$

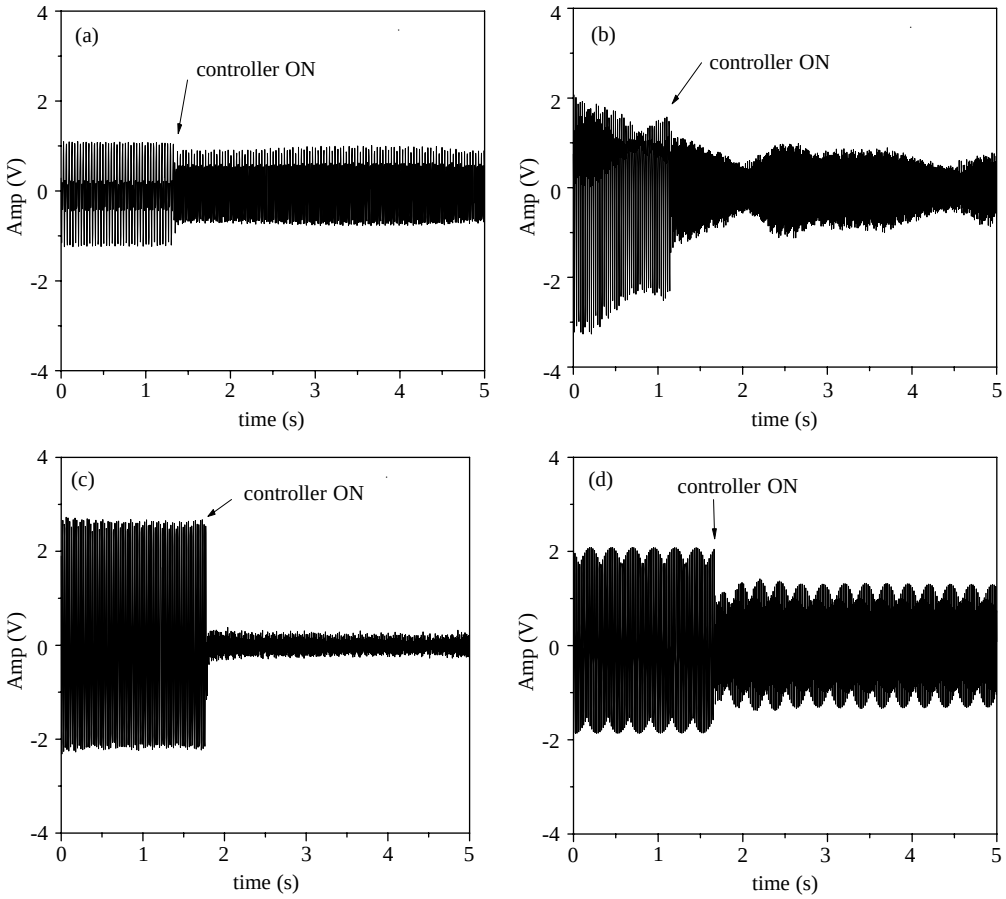

Fig. 10. The time histories of the sensor S1 at different modal frequencies (adaptive feedforward control): (a) at the first modal frequency, (b) at the second modal frequency, (c) at the third modal frequency, (d) at the fourth modal frequency.

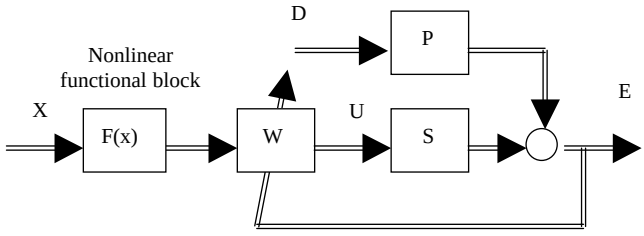

Fig. 11. Adaptive non-linear control.

where a_i and NN are the coefficients and the order of the polynomial. Control signals in Eq. (4) can then be changed as

$$u_j(k) = \sum_{l=1}^{L} w_{jl} f(x, a_i, k - l + 1). \tag{11}$$

Substituting Eq. (11) into Eq. (3) results in

$$e_i(k) = \sum_{m=1}^{M} p_i(m)d(k-m+1) + \sum_{j=1}^{4}\sum_{n=1}^{N} s_{ij}(n)\sum_{l=1}^{L} w_{jl}f(x,a_i,k-n-l+2)$$
$$= \sum_{m=1}^{M} p_i(m)d(k-m+1) + \sum_{j=1}^{4}\sum_{l=1}^{L} w_{jl}r'_{ij}(k-l+1), \tag{12}$$

where

$$r'_{ij}(k) = \sum_{n=1}^{N} s_{ij}(n)f(x,a_i,k-n+1). \tag{13}$$

The recursive LMS algorithm can be denoted as

$$w_{jl}(k+1) = w_{jl}(k) + \mu\frac{\partial J(k)}{\partial w_{jl}}, \tag{14}$$

$$\frac{\partial J(k)}{\partial w_{jl}} = 2\sum_{i=1}^{4} e_i(k)r'_{ij}(k-l+1). \tag{15}$$

An evident question is how to determine the coefficients a_i in the polynomial. If they are not properly determined, the control algorithm may be difficult to be made stable. A simple and effective method adopted here is that of setting these coefficients on-line. Generally, for harmonic vibration control, the required order of the polynomial is low, for example, the fourth order polynomial is enough for the considered plate vibration reduction.

The adaptive non-linear control can be simplified as adaptive feedforward control, if $a_1 = 1$ and $a_i = 0$ $(i = 2, 3, 4, \ldots, NN)$ in Eq. (10).

Fig. 12 shows the responses of the sensor S1 under the sinusoidal excitations at the first four modal frequencies, respectively, using the adaptive non-linear control. It can be easily seen that these results are much better than those shown in Fig. 10, though the non-linearity of the plate causes higher harmonic components in these responses. Table 1 also indicates that the harmonic components of interest (below 200 Hz) are fully suppressed by the adaptive non-linear controller (ANC). For example, while the plate is excited by a sinusoidal signal at the first plate modal frequency, the fundamental, the second, third and fourth harmonic components of the sensor S1 decrease by 86, 50, 38, and 13 dB, respectively. The responses of the sensors S2–S4 demonstrate the same results.

Fig. 13 illustrates the vibration reduction of the sensors S1–S4 in the case of a swept-frequency harmonic excitation from 0 to 100 Hz. Table 2 shows the amplitude of the power spectrum of each sensor at six modal frequencies. The amplitudes are decreased on average by 11.1, 18.1, 18.8, 20.9, 17.0, 4, and 20.1 dB, respectively. This figure also shows that a small control is obtained between 70–80 Hz where a vibration mode is present. It is mainly due to the fact that the decentralized adaptive non-linear control strategy is under the assumption that the collocated sensors and actuators predominate, but this assumption is not satisfied well in this frequency range as shown in Fig. 5.

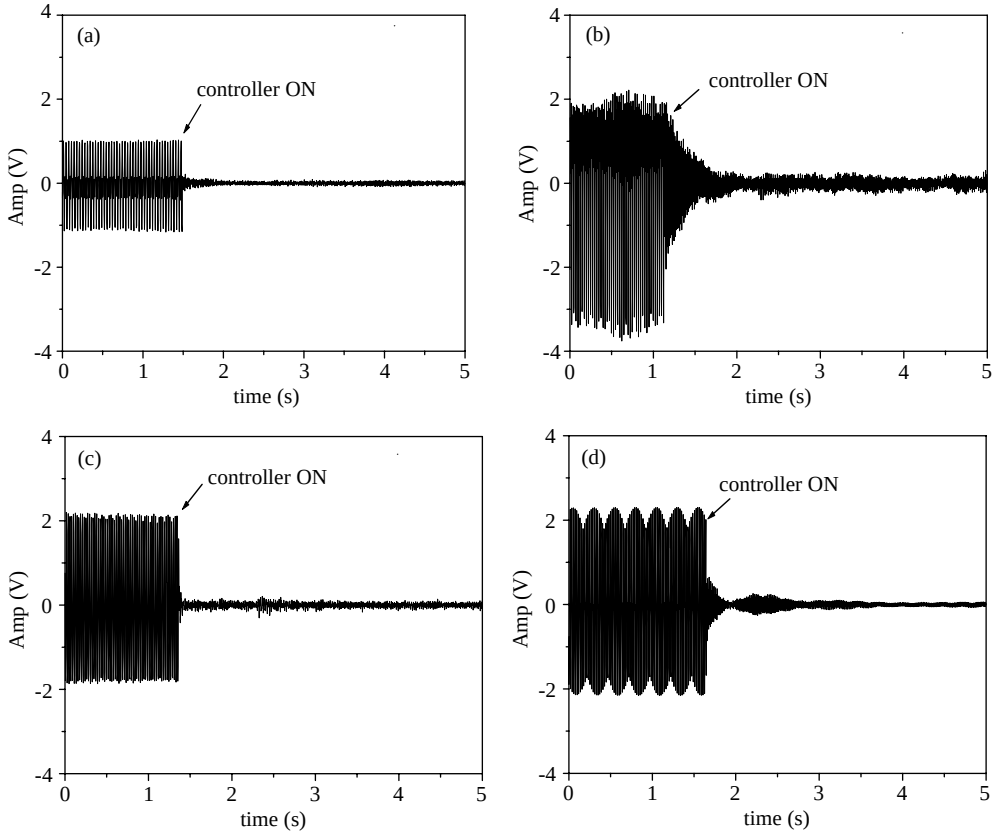

Fig. 12. The time histories of the sensor S1 at different modal frequencies: (adaptive non-linear control): (a) at the first modal frequency, (b) at the second modal frequency, (c) at the third modal frequency, (d) at the fourth modal frequency.

Table 1
The amplitudes of power spectra in dB

Frequency (Hz)	Fundamental			The second harmonic			The third harmonic			The fourth harmonic		
	UC	AFC	ANC	UC	AFC	ANC	UC	AFC	ANC	UC	AFC	ANC
26	−13.6	−90	−100	−43	−41.7	−92	−62.2	−63.8	−100	−60.3	−59.5	−73
37.5	−15.2	−88	−80	−27.2	−25.4	−77	−33.6	−31.2	−73	−36.4	−33.1	−47
42	3.4	−90	−90	−29	−31	−67	−44.6	−44	−50	−37.4	−34.9	−37.4
52.5	3.7	−90	−80	−14.8	−16.8	−68	−34	−36	−53	−37	−44	−49.3
63	−4.4	−90	−90	−29.7	−41.4	−58	−45.7	−55.5	−51.3	−54.2	−65.5	−67
83	0.8	−89	−90	−15.4	−13.7	−47	−41.5	−41.6	−40.6			
89.5	−6.8	−90	−90	−31.5	−49	−68						
103	−10	−90	−90	−30	−32.8	−32						
110	−3.2	−85	−85									

Note: UC: uncontrolled AFC: adaptive feedforward control ANC: adaptive non-linear control.

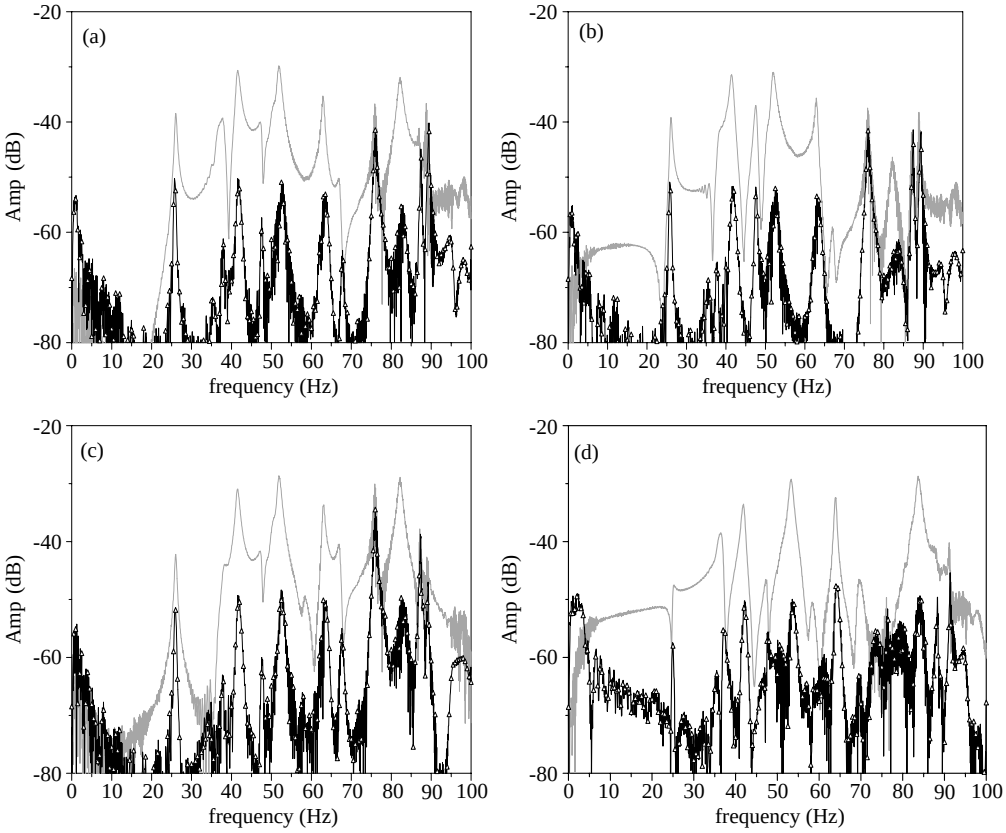

Fig. 13. The spectra of different sensors for a swept-frequency harmonic excitation: (a) sensor S1, (b) sensor S2, (c) sensor S3, (d) sensor S4; ——, without control; —△—, with control.

Table 2
The response spectrum amplitudes of different sensors in dB

Frequency (Hz)		25	36	42	53	64	76	84
Sensor S1	Uncontrolled	−38.0	−39.0	−30.4	−29.9	−35.5	−36.4	−31.9
	Controlled	−50.2	−61.4	−50.0	−51.3	−53.3	−41.2	−55.1
	Difference	12.2	22.4	19.6	21.4	17.8	4.8	23.2
Sensor S2	Uncontrolled	−39.4	−51.2	−30.9	−30.7	−35.7	−37.1	−46.4
	Controlled	−50.0	−65.5	−51.7	−52.3	−53.8	−41.5	−61.2
	Difference	11.6	14.3	20.8	21.6	18.1	4.4	14.8
Sensor S3	Uncontrolled	−41.7	−43.8	−30.9	−28.4	−33.7	−30	−28.6
	Controlled	−51.7	−62.7	−48.9	−47.9	−50.0	−34.3	−50
	Difference	10.0	18.9	18.0	19.5	16.3	4.3	21.4
Sensor S4	Uncontrolled	−47.1	−38.3	−33.5	−28.9	−32.2	−49.2	−28.6
	Controlled	−57.6	−55.0	−50.0	−50.0	−47.7	−51.6	−49.5
	Difference	10.5	16.7	16.5	21.1	15.5	2.4	20.9

4. Conclusions

In this paper, the dynamic behavior, control and experiment of a clamped rectangular plate with bonded piezoelectric ceramic patches are investigated. The plate exhibits dense modes, varying inherent characteristics and non-linearity. An adaptive non-linear control scheme is proposed which introduces a non-linear function into the adaptive feedforward control to non-linearize the reference signal. Both adaptive feedforward control and the adaptive non-linear control are realized in the dSPACE real-time control system, and the vibration reduction is compared for both controllers in the cases of sinusoidal excitations with the first nine modal frequencies of the plate, and a swept-frequency harmonic excitation. The evident higher harmonic vibration reduction of the adaptive non-linear control scheme demonstrates its validity and reliability.

Acknowledgements

This work is part of the leading project ADAPTRONIC financially supported by the German Ministry of Research and Technology. The author acknowledges the support of DLR during the research period. Meanwhile, the author would like to thank Dr. Mehrdad N. Ghasemi Nejhad of the University of Hawaii at Manoa for his understanding during the preparation of this paper.

References

[1] I. Bar-Kana, K. Howard, Simple adaptive control of large flexible space structures, IEEE Transactions on Aerospace and Electronic Systems 29 (1993) 1137–1149.
[2] B. Widrow, J.R. Glover, J.M. McCool, J. Kaunitz, C.S. Williams, R.H. Hearn, J.R. Zeidler, E. Dong, R.C. Goodlin, Adaptive noise canceling: principles and application, Proceedings of the IEEE 63 (1975) 1692–1716.
[3] P.A. Nelson, S.J. Elliott, Active Control of Sound, Academic Press, London, 1992.
[4] H.T. Russell, A.B. Rixardo, A.L. Steven, Time-averaged active controller for turbofan Engine fan noise reduction, Journal of Aircraft 33 (1996) 524–531.
[5] J. Melcher, R. Wimmel, Modern adaptive real-time controllers for actively reacting flexible structures, Journal of Intelligent Material Systems and Structures 2 (1991) 328–346.
[6] R.A. Burdisso, E. Suarez, C.R. Fuller, Feasibility study of adaptive control of structures under seismic excitation, American Society of Civil Engineers Journal of Engineering Mechanics 120 (1994) 580–591.
[7] K.G. Ma, Z.Q. Gu, F.J. Peng, X. Chen, On experiments of adaptive control for structure vibration, Proceedings of the ASME 16th Biennial Conference on Mechanical Vibration and Noise and 1997 ASME Design Technical Conferences, Paper number DETC97/VIB-3939, Sacramento, CA, 1997.
[8] K.G. Ma, Z.Q. Gu, Adaptive control for structural response of helicopters, Acta Aeronautica et Astronautica Sinica 18 (3) (1997) 359–362.
[9] I.D. Roy, W. Eversman, Adaptive flutter suppression of an unswept wing, Journal of Aircraft 33 (1996) 775–783.
[10] K.G. Ma, J. Melcher, The comparison of different control strategies for reducing vehicle vibration, German Aerospace Center, IB 131–99/41, 1999, pp. 1–28.
[11] R. Lammering, S. Wiesemann, L.F. Campanile, J. Melcher, Design, optimization and realization of smart structure, Smart Materials and Structure 9 (2000) 260–266.
[12] Y. Lim, S.V. Gopinathan, V.V. Varadan, V.K. Varadan, Finite element simulation of smart structures using an optimal output feedback controller for vibration and noise control, Smart Materials and Structure 8 (1999) 324–337.

[13] S.Y. Hong, V.V. Varadan, V.K. Varadan, Implementation of coupled mode optimal structural vibration control using approximated eigenfunctions, Smart Materials and Structure 7 (1998) 63–71.
[14] C. Chen, Y. Shen, Optimal control of active structure with piezoelectric modal sensors and actuators, Smart Materials and Structure 6 (1997) 403–409.
[15] X. Shen, A. Homaifar, Vibration control of flexible structures with PZT sensors and actuators, Journal of Vibration and Control 7 (2001) 417–451.
[16] C. Chantalakhana, R. Stanway, Active constrained layer damping of plate vibrations: a numerical and experimental study of modal controllers, Smart Materials and Structure 9 (2000) 940–952.
[17] A. EI-Sinawi, R. Kashani, Active vibration isolation of plate structures using a Kalman estimator-based feedforward controller, ASME DE-Vol.97/DSC-Vol.65, 1998, pp. 173–178.
[18] M. Maertens, H. Waller, Vibration control of a plate structure with piezoelectric stack actuators, Proceedings of the SPIE Conference on Smart Structure and Integrated Systems, Newport Beach, CA, 1999, pp. 738–746.
[19] J.P. Melian, S. Homann, H.P. Monner, Experimentalle Untersuchungen von Platten mit applizierten PZT-Funktionsmodulen hinsichtlich ihres dynamischen Verhaltens, German Aerospace Center, IB131-2001/07, 2001.
[20] K.G. Ma, J. Melcher, H.P. Monner, Study on adaptive control strategies for smart structure vibration suppression, Proceedings of the 11th International Conference on Adaptive Structures and Technologies, Nagoya, Japan, 2000, pp. 447–454.